Mechanism of Calcium Carbonate Scale Deposition on Heat-Transfer Surfaces

ARTICLE *in* INDUSTRIAL & ENGINEERING CHEMISTRY FUNDAMENTALS · FEBRUARY 1968

DOI: 10.1021/i160025a011

5 AUTHORS, INCLUDING:

David Hasson
Technion - Israel Institute of Technology
101 PUBLICATIONS **2,206** CITATIONS
SEE PROFILE

Mordecai Avriel
Technion - Israel Institute of Technology
72 PUBLICATIONS **1,803** CITATIONS
SEE PROFILE

MECHANISM OF CALCIUM CARBONATE SCALE DEPOSITION ON HEAT-TRANSFER SURFACES

DAVID HASSON, MORDECAI AVRIEL,[1] WILLIAM RESNICK, TZVI ROZENMAN,[2] AND SHLOMO WINDREICH

Department of Chemical Engineering, Technion–Israel Institute of Technology, Haifa, Israel

$CaCO_3$ scale deposition rates were accurately measured using an annular constant heat-flux exchanger which maintains the reaction surface at constant temperature, irrespective of scale layer thickness. The separate effects of flow velocity, scale surface temperature, and water composition were examined according to the rate model presented. Within the range of surface temperatures (67° to 85° C.) and Reynolds numbers (13,000 to 42,000) investigated, $CaCO_3$ deposition is mainly controlled by the forward diffusion rate of Ca^{+2} and HCO_3^- ions. In certain cases, it is also controlled by the backward diffusion rate of dissolved CO_2 formed during the reaction.

SCALE deposition, which occurs on the tube walls of a heat exchanger during the flow of water containing dissolved scale constituents, is a complex crystallization process. Because the scale constituents [$CaCO_3$, $Mg(OH)_2$, $CaSO_4$] have solubilities which diminish with increasing temperature, the solution in contact with the heat-transfer surface has the lowest equilibrium solubility. Scale tends, therefore, to deposit on the heat-transfer surface when local supersaturation conditions exist in its vicinity.

The rate of formation of an initial scale layer and its rate of growth are determined by the interaction of several rate processes: nucleation, diffusion, chemical reaction, and molecular ordering of the scale crystal lattice. To control scale formation, it is necessary to have a quantitative understanding of the relative importance of the individual rate processes and to relate rate of scale growth with the significant operating parameters.

The object of this study was to elucidate the controlling rate mechanisms in the deposition of $CaCO_3$ scale during the turbulent flow of nonboiling hard water in contact with a heat-transfer surface. A previously proposed model (Hasson, 1962) was extended and verified by more accurate data on rate of scale growth, obtained with an improved experimental technique for scale research, developed as part of this study.

Rate Model for $CaCO_3$ Crystallization

The over-all reactions occurring in the crystallization of $CaCO_3$ scale are represented by:

$$2\,HCO_3^{-2} \underset{k'}{\overset{k}{\rightleftharpoons}} CO_3^{-2} + CO_2 + H_2O \qquad (1)$$

$$Ca^{+2} + CO_3^{-2} \xrightarrow{k_R} CaCO_3\,(s) \qquad (2)$$

For the sake of brevity, these reactions are denoted as follows:

$$2\,F \underset{k'}{\overset{k}{\rightleftharpoons}} M + E + H_2O \qquad (1a)$$

$$B + M \xrightarrow{k_R} BM \qquad (2a)$$

When $CaCO_3$ scale deposits on the tube wall of a heat exchanger, the first layer is formed on a metallic surface while subsequent layers grow on $CaCO_3$ crystals. Experiments show that nucleation of $CaCO_3$ on the metallic surface occurs at a rate which is not significantly different from that of the subsequent growth on $CaCO_3$ crystals. The contrast, prominently displayed by $CaSO_4$ scale, between a relatively slow initial nucleation on the metallic surface and a subsequent more rapid growth on $CaSO_4$ crystals, is not evident with $CaCO_3$.

Therefore, only the growth process of $CaCO_3$ scale on a heat-transfer surface already coated with an initial scale layer is considered and the object is to formulate an over-all rate equation in terms of the significant operating parameters. Assuming turbulent flow, the radial temperature profile may be schematically represented as in Figure 1. Depending on the local heat flux, dq/dA, and the liquid side film coefficient for heat transfer, h_f, the scale-liquid interface will be at a temperature T_s, which is higher than the liquid bulk temperature, T_b (Equation 7). As long as the bulk water composition is such that the equilibrium $CaCO_3$ solubility, C^*, at the scale surface temperature, T_s, is exceeded, an over-all concentration difference ($C - C^*$) will act to drive the chemical and physical processes leading to the growth of the scale layer.

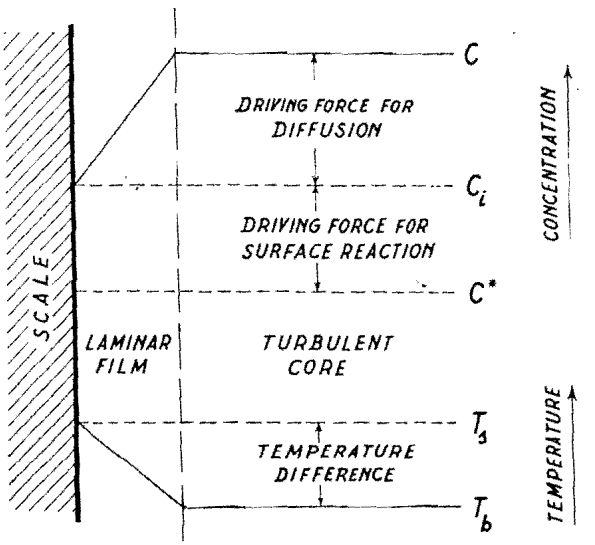

Figure 1. Radial temperature and concentration profiles

[1] Present address, Central Research Department, Mobil Oil Co., Princeton, N. J.
[2] Present address, Department of Chemical Engineering, Illinois Institute of Technology, Chicago, Ill.

Reprinted from I&EC FUNDAMENTALS, Vol. 7, Page 59, February 1968

To formulate an over-all rate equation for this heterogeneous reaction, the growth of the $CaCO_3$ scale layer may be conceived to occur according to the following steps:

Diffusion of the reactants Ca^{+2} and HCO_3^- from the water bulk toward the scale-liquid interface. The rate coefficients for diffusion of these ions are k_B and k_F, respectively, and since electrical neutrality must be preserved, it follows that $k_F = k_B = k_{BF}$.

Chemical reaction at the scale interface, leading to the formation of CO_3^{-2} and CO_2 (Equation 1). The rate coefficients for this reversible reaction, assumed to be of second order, are k in the forward direction and k' in the reverse direction.

Crystallization of $CaCO_3$ on the scale surface. The process in which freshly formed $CaCO_3$ molecules order themselves into the crystal lattice is taken to be a first-order reaction with a rate coefficient k_R.

Diffusion of the reaction product, dissolved CO_2, from the reaction surface toward the water bulk. The rate coefficient for the backward diffusion of dissolved CO_2 toward the water bulk is k_E. In a limiting case, where the CO_2 formed is rapidly released in gaseous form at the reaction surface, $1/k_E = 0$.

By equating the rates of the individual processes described above, a set of equations is obtained, from which the unknown concentrations at the reaction surface may be eliminated. The over-all rate of $CaCO_3$ deposition, in moles per unit area per unit time, is:

$$w/k = (C_F - 2\,w/k_{BF})^2 - (K_1'/K_2') \cdot (C_E + w/k_E) \cdot \left[w/k_R + \frac{K'_s}{C_B - w(1/k_{BF} + 1/k_R)} \right] \quad (3)$$

Equation 3 embodies the effects of the three basic operating parameters which determine the rate of scale deposition: water composition, scale surface temperature, and flow conditions (Reynolds number). The effect of water composition is expressed by the bulk concentrations of the bicarbonate ion (C_F), calcium ion (C_B), and dissolved CO_2 (C_E). Concentrations C_F and C_E can be readily calculated by the well known equilibrium relationships of the carbonate system (Hamer *et al.*, 1961), from chemical analysis of the water alkalinity, pH value, and total dissolved solids content.

The effect of scale surface temperature enters in two ways: through the $CaCO_3$ solubility product, K'_s, which diminishes with increasing temperature, and through the temperature dependence of the chemical rate coefficients, k, k', and the crystallization rate coefficient, k_R. These rate coefficients increase with temperature according to the Arrhenius law, and are independent of flow variables.

The effect of flow conditions is expressed by the dependence of the diffusion rate—i.e., mass transfer coefficients k_{BF} and k_E—on Reynolds number.

A critical test that may be applied to verify the above model is to compare the experimentally determined mass transfer coefficient, k_{BF}, for diffusion of the calcium bicarbonate ions with the measured film coefficient for heat transfer, h_i. According to the j-factor analogy between heat and mass transfer, the rate coefficients for simultaneous heat and mass transfer must satisfy the following relationship:

$$k_{BF}/h_i = (1/C_p\rho) \cdot (\mathrm{Pr}/\mathrm{Sc})_f^{2/3} \quad (4)$$

where Pr and Sc are the Prandtl and Schmidt numbers of the solution, taken at the average film temperature.

Equation 4 shows that the diffusion rate coefficients for CO_2 and calcium bicarbonate are related to each other by:

$$k_{BF}/k_E = (\mathrm{Sc}_E/\mathrm{Sc}_{BF})_f^{2/3} \quad (5)$$

Determination of Scale-Deposition Rate with Constant Heat-Flux Exchanger

The rate of scale growth is best measured accurately under conditions such that the scale layer grows linearly with time. To obtain a constant rate of scale growth with water of nonvarying composition and flow rate, it is also necessary to hold the scale surface at a fixed temperature which does not vary with the thickness of the growing scale layer. This requirement is achieved in a constant flux heat exchanger, as shown below.

Consider scale growth on the heat-transfer surface of an exchanger supplied with a constant and uniform heat flux, $dq/dA = q/A$, such as may be obtained with an electrical heating element inside a tube. At a measurement section situated downstream, water of inlet temperature T_1 and flow rate W' will have reached a bulk temperature T_b and the scale-water interface will be at a temperature T_s, given by:

$$\frac{q}{A} = \frac{W'}{A} \cdot C_p \cdot (T_b - T_1) = \text{const.} \quad (6)$$

$$\frac{dq}{dA} = h_t \cdot (T_s - T_b) = \frac{q}{A} = \text{const.} \quad (7)$$

Since the flow velocity is maintained constant, film coefficient h_i depends only on physical properties, all of which are temperature-dependent. Accordingly, h_t may be expressed in the following general form:

$$h_t = f(T_s, T_b) \quad (8)$$

Inspection of Equation 6 shows that T_b must remain constant, and Equations 7 and 8 show that h_t and T_s are also constant, irrespective of scale-layer thickness. It follows that the rate of scale growth at the section considered remains constant with time, and is practically uniform along the tube when bulk temperature rise is small.

The magnitude of the scale-growth rate may be experimentally determined by recording the tube wall temperature, T_o, and the water bulk temperature, T_b. The radial temperature drop $(T_o - T_b)$ arises from two resistances, one due to the scale layer and the other due to the water film. Thus,

$$\frac{dq}{dA} = \frac{q}{A} = \frac{T_o - T_b}{(x/k_s) + (1/h_t)} = \text{const.} \quad (9)$$

from which it follows that w, the scale-growth rate (in weight per unit time per unit area), is given by:

$$w = \rho_s \cdot \frac{dx}{dt} = \frac{\rho_s A k_s}{q} \cdot \frac{d(T_o - T_b)}{dt} = \text{const.} \quad (10)$$

where $d(T_o - T_b)/dt$ is the slope of the straight line representing the variation of the temperature difference $(T_o - T_b)$ with time. The temperature of the tube at time $t = 0$ before a scale layer has formed on the tube is the temperature, T_s, of the scale-water interface.

Experimental

Figure 2 shows a schematic diagram of the flow system and Figure 3 describes the electrical system. Water of a desired composition was continuously circulated through an electrically heated double-pipe exchanger. In passing through the annular passage of the exchanger, water coming in contact with the internally heated central section of the inner pipe deposited a layer of scale on it.

Heat Exchanger. Details of the double-pipe exchanger are shown in Figure 4.

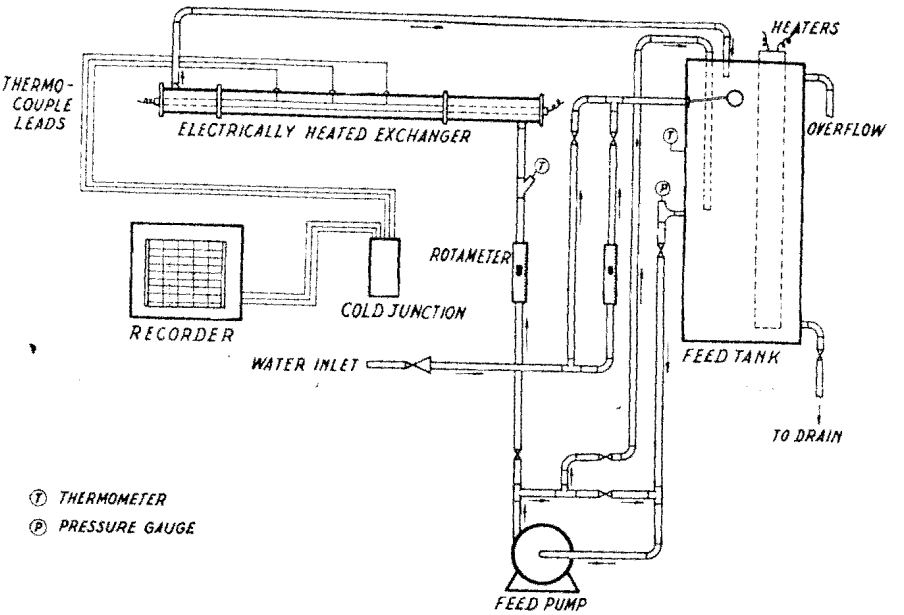

Figure 2. Schematic diagram of flow system

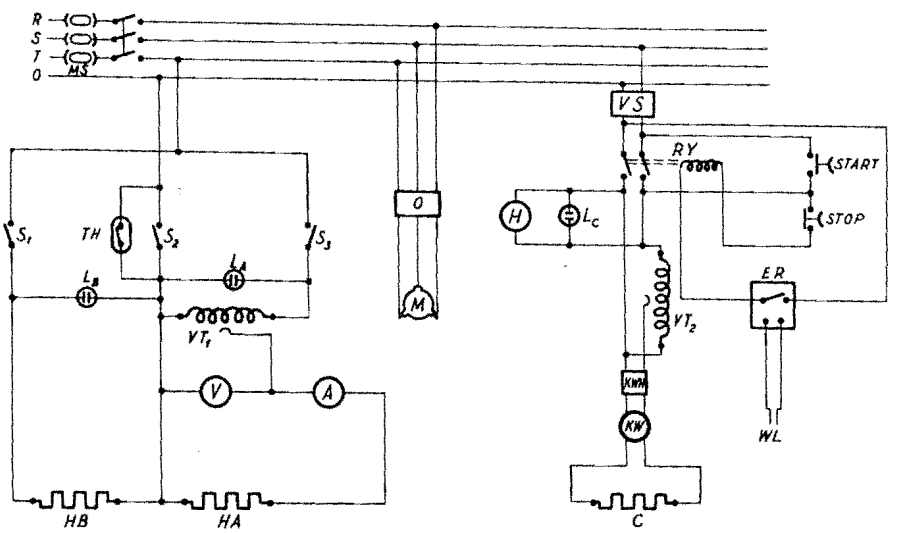

Figure 3. Wiring diagram of electrically heated exchanger system

A. Ammeter
C. Heating element of electrical exchanger
ER. Electronic relay
H. Hourmeter
HA, HB. Electrical heating elements in feed water tank
KW. Kilowatt-hour meter
LA, LB. Control lamps
M. Motor of feed pump
MS. Main switch
O. Feed pump motor switch
RY. Relay
S_1, S_2, S_3. Switches
TH. Thermoswitch in feed woter tank
V. Voltmeter
VS. Voltage stobilizer
VT_1, VT_2. Variacs
WL. Electrodes immersed in water

The main part of the outer pipe (38.1-mm. i.d.) consisted of a thick-walled Perspex tube which allowed visual observation of the scale deposition process and also served as a heat insulator. The inner pipe was made of three pieces of copper tubing (12.7-mm. o.d.) representing, respectively, an unheated entry section, a 610-mm. long test section enclosing the heating element, and an unheated exit section. To prevent axial heat losses from the ends of the heated test section, the three copper tubes were interjoined by screwing with two Textolite heat-insulating tubes having the same outside diameter.

Two perforated Ebonite disks, located near the inlet and the outlet of the flow channel, served to center the inner pipe and to smooth the flow. The entry length provided for development of the flow profile from the inlet disk to the edge of the test section, corresponded to 20 equivalent diameters. The distance from the edge of the test section to the thermocouples represented the entry length for the development of the heat and mass transfer boundary layers. This distance varied between 6 and 18 equivalent diameters for the respective thermocouples.

The electrical element consisted of 1-mm. coil-wound Nichrome wire, housed inside a quartz tube (8.3-mm. o.d., 5.6-mm. i.d.) which provided electrical insulation from the copper tube. Elements were designed to supply up to 3.7 kw. at full load (220 volts). The short lifetime of an element under high-load conditions was prolonged by passing through the quartz tube a very slow nitrogen stream so as to prevent oxidation of the Nichrome wire.

Temperature Measurements. The wall temperature of the heated copper tube and the corresponding water bulk temperature were measured by means of thermocouple pairs situated at three equally spaced locations along the test section. To minimize a possible measurement error from the flow disturbance caused by the thermocouple leads, each wall

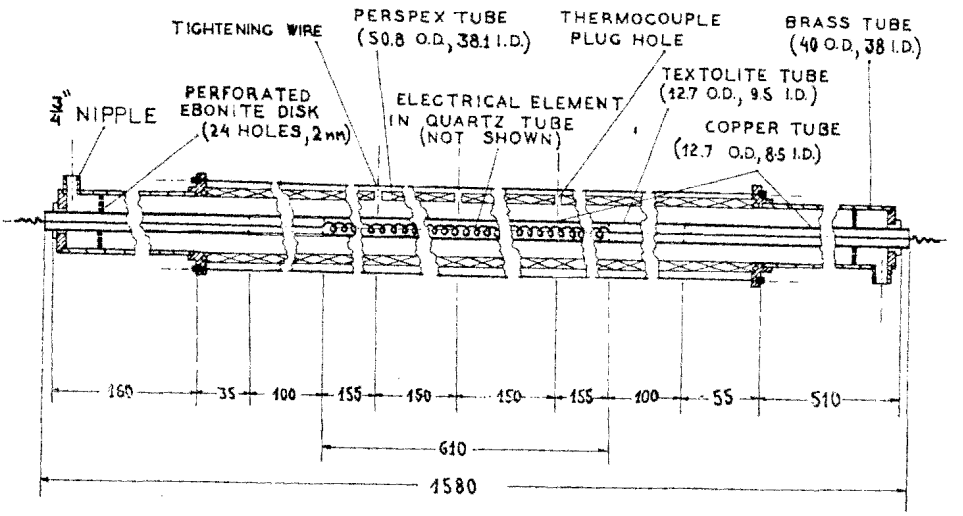

Figure 4. Electrically heated exchanger

All dimensions in mm.

thermocouple was soldered into a spiral groove shaped such that the leads issued in a position diametrically opposite the location of the thermocouple junction. The error was further minimized by employing miniature thermocouples, manufactured by Baldwin-Lima Hamilton (Type TCC-IAG-200 consisting of copper-constantan wire, 0.0001 inch in diameter, protected by a sheath 0.014 inch in o.d.). The temperature readings were recorded on a Bristol Dynameter six-point recorder having a span of 0.5 mv. and a precision of ± 0.025 mv.

Water Supply. The water entering the exchanger had to be preheated to achieve sufficiently high surface temperatures. Recirculating water was therefore kept in the feed tank at about 40° C., regulated to a constant value within ± 1° C. Preheat temperatures exceeding 45° C. were not attempted, so as not to risk scale precipitation in the water bulk.

The make-up and blown-down streams were each maintained at a flow rate of about 1.5 liters per minute, capable of removing from the system a heat quantity slightly in excess of the exchanger heat input. The scale removal rate, by deposition in the exchanger, was small compared with the rate of addition of scaling salts brought into the system by the make-up stream.

Make-up water was fed from the municipal supply. When so desired, the tap water was mixed with $CaCl_2$ or $NaHCO_3$ to increase the scaling tendency or, in the opposite case, was diluted with distilled water. A 6-cu. meter storage system became available for the latter part of this study. It enabled a whole run to be carried out with the same batch of make-up water and provided the best controlled data.

Operating Data and Scale Properties. Experimenta runs extended over 16 to 60 hours the time necessary to obtain sufficient points for drawing a reliable straight line through the readings of temperature difference ($T_s - T_b$) *vs.* time. Typical results of the temperature-difference variation with time are shown in Figure 5. The initial points deviating from the straight line represent the time necessary for bringing the system into steady state and for nucleation on the scale-free metal surface. This startup period was less than 2 to 4 hours, showing that surface nucleation with $CaCO_3$ scale is relatively rapid.

The rise in water bulk temperature across the exchanger was less than 3° C., so that surface temperature could be considered to be substantially constant along the heated length of the exchanger. Figure 6 shows typical measurements of the scale thickness along the heated length of the exchanger at the end of a run. The end effects should have little influence on the accuracy of the measurements, since the thermocouple probes were located well within the uniform-deposition part of the exchanger.

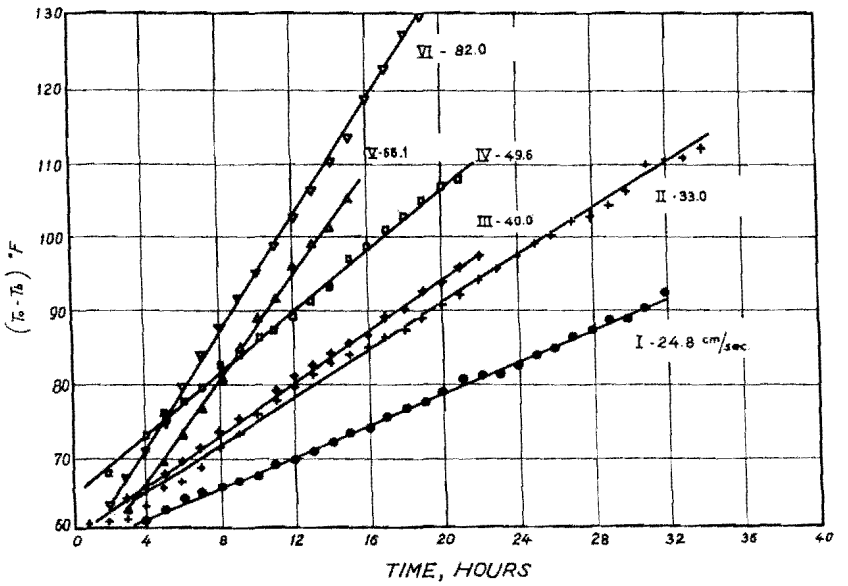

Figure 5. Temperature difference variation with time in velocity effect runs

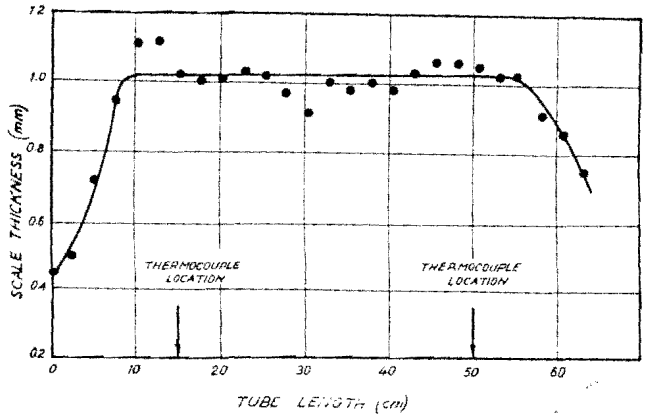

Figure 6. Scale thickness at end of run

Although the water also contained magnesium hardness, the scale was composed of almost pure $CaCO_3$, analyzing over 99% $CaCO_3$. Crystallographic analyses of a few scale samples indicated predominance of the aragonite form, but no generalization can be made because of lack of sufficient data.

Scale thermal conductivities were obtained from measurement of the scale thickness at the end of a run. The average value of k_s = 1.45 kcal./hr. meter ° C. was adopted for calculation of the scale-growth rate from Equation 10. The average value of scale density was ρ_s = 2.76 grams per cc.

The authors initially thought that the scale removal method (mechanical filing or dissolution by acid solution containing an inhibitor) had an effect on the initial scale growth rate. This was disproved by the experimental evidence.

Results

The main results were obtained in three series of experiments designed to investigate the separate effects of flow velocity, scale surface temperature, and water composition on rate of scale growth.

Effects of Velocity and Surface Temperature. The effect of velocity on scale-growth rate was investigated over the range of 25 to 82 cm. per second. Surface temperature was held substantially constant within the range of 75° to 76.5° C. and bulk water temperature was at 45° ± 0.8° C. The recirculating water analyzed as follows:

pH	7.35 to 7.5
Calcium	300 to 320 p.p.m. as $CaCO_3$
Total alkalinity	300 to 350 p.p.m. as $CaCO_3$
Total dissolved solids	600 to 750 p.p.m.

Results (Figures 5 and 7) showed a pronounced dependence of velocity on rate of scale growth. A plot of the scale-growth rate, w (grams of $CaCO_3$ per hour per square meter), as a function of Reynolds number (Figure 7), gave a straight line which is represented by the following equation:

$$w = 0.054\ (\mathrm{Re})_f^{0.68} \qquad (11)$$

Measurements of the heat-transfer coefficient, h_t, over the same range of the variables, obtained with nonscaling soft water flowing in the exchanger, yielded:

$$\frac{h_t\, d_e}{k_w} = 0.0608\ (\mathrm{Re})_f^{0.716} \cdot (\mathrm{Pr})_f^{1/3} \qquad (12)$$

The Reynolds number power 0.68, obtained from mass-transfer data, is very close to the power 0.72, deduced from heat-transfer data, though both values are somewhat lower than the 0.8 power expected for fully developed turbulent flow.

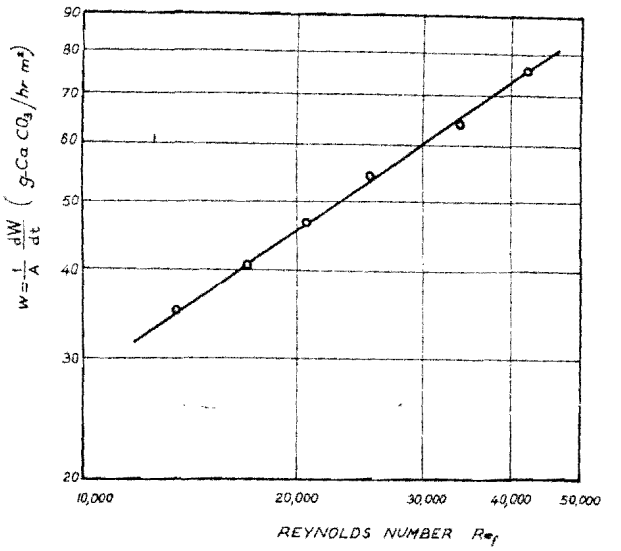

Figure 7. Effect of Reynolds number on rate of growth

The deviation from the 0.8 power is probably due to insufficient entrance length for development of the thermal and mass-transfer boundary layers. There is scanty information on heat and mass transfer in the entrance region of annuli. Fluid function data (Rothfus *et al.*, 1955) indicate that the Reynolds power in the entrance region should have a value lower than 0.8, as found here.

The close similarity between the Reynolds number powers, found for both heat-transfer and scale-growth rates, suggests that diffusional mechanisms are dominant in the temperature range under consideration. Results for the effect of surface temperature on scale-growth rate are consistent with this hypothesis. Figure 8 shows the variation of growth rate with surface temperature, measured with water flowing at constant velocity of 49.6 cm. per second and having substantially identical composition and bulk temperature as in the velocity tests.

The increase of growth rate with surface temperature is relatively slow, amounting to only 20% when the temperature is raised from 67.5° to 82.5° C. This slow increase can be accounted for by the decreasing solubility of $CaCO_3$ and the small increase of mass transfer coefficients with temperature.

Predicted and Observed Growth Rates. The experimental correlation of the data on growth rate (Equation 11) can be compared with an expression predicted by the proposed

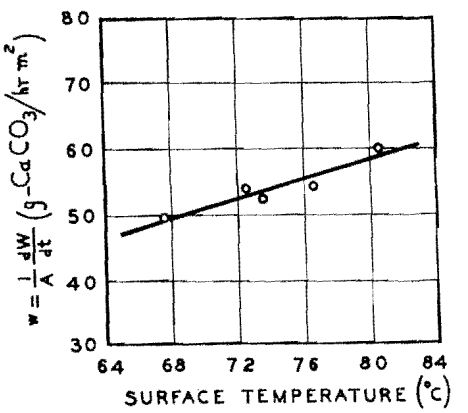

Figure 8. Effect of temperature on rate of growth

rate model. For diffusion-controlled scale growth, Equation 3 simplifies as follows:

$$(C_E + w/k_E) = (K_2'/K_3' \cdot K_3') \cdot (C_F - 2\,w/k_{BF})^2 \cdot (C_B - w/k_{BF}) \quad (13)$$

As discussed below, conditions in the above test series were such that $1/k_E = 0$. On inserting concentrations of the average water composition during these tests, Equation 13 gives:

$$w/k_{BF} = C_B - C_{Bi} = 260 \text{ p.p.m. as } CaCO_3 \quad (14)$$

The dependence of the mass transfer coefficient, k_{BF}, on Reynolds number can be estimated from the heat-transfer correlation (Equation 12), by applying the j-factor analogy between heat and mass transfer (Equation 4). On combining Equations 4, 12, and 14 and inserting numerical values for the parameters held constant in the tests considered, the assumption of diffusion-controlled scale growth predicts the following result:

$$w = 0.03\ (\mathrm{Re})_f^{0.716} \quad (15)$$

The close similarity between this prediction and the observed results given by Equation 11 demonstrates the validity of the proposed model.

Effects of Water Composition. The main and best controlled experiments for studying the effect of water composition were carried out with batches of constant composition water prepared in the 6-cu. meter storage reservoirs. The concentrations of dissolved scale constituents in the different tests were varied within the following range:

pH	7.5 to 7.8
Calcium	110 to 575 p.p.m. as $CaCO_3$
Total alkalinity	130 to 320 p.p.m. as $CaCO_3$
Total dissolved solids	320 to 1250 p.p.m.

Scale surface temperature was held constant within the range of 80° to 85° C. while bulk water temperature was fixed at either 35° or 43° C. The flow velocity was 25.5 cm. per second in all cases.

The average value of the measured film coefficient for heat transfer in the above experiments was $h_f = 2190$ kcal./hr. sq. meter ° C. The j-factor analogy (Equation 4) predicts for these constant Reynolds number experiments a mass transfer coefficient of $k_{BF} = 0.128$ meter per hour = 0.128 gram of $CaCO_3$/hr. sq. meter Δ p.p.m. $CaCO_3$, and from Equation 5, $k_E/k_{BF} = 1.6$. Predicted and experimental values can be compared by plotting the measured rate of scale growth against the calcium-concentration driving force, $w/k_{BF} = C_B - C_{Bi}$, calculated from Equation 13 for the corresponding bulk water composition. All data should fall on a straight line having a slope of k_{BF} and passing through the origin. This comparison is shown in Figure 9. Neglecting for the moment runs 36, 39, 40, and 41, which pertain to the highest concentrations, and run 42, which relates to the most dilute solution, the straight-line correlation of the data gives a slope of $k_{BF} = 0.115$, which is close to the anticipated value of 0.128.

Diffusional Resistance of CO_2. The deviation of run 42, relating to a highly diluted solution ($C_B = 112$ p.p.m., $C_F = 136$ p.p.m. as $CaCO_3$), is readily explained by the neglect of the surface nucleation step in the proposed analysis. At sufficiently low supersaturations, nucleation becomes a significant factor. In fact, deviations from the straight line of Figure 9 are expected for low values of the concentration difference driving force (Van Hook, 1961).

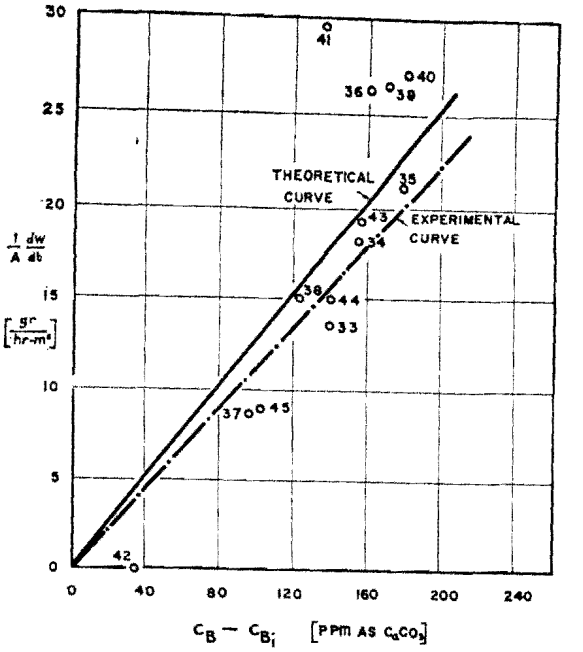

Figure 9. Effect of concentration on rate of growth

The deviation in the high concentration runs may be explained by one of two effects: bulk precipitation which can contribute to increased scale growth on the wall or escape of gaseous CO_2 on the reaction surface under high supersaturation conditions. The former explanation holds only for run 41, which differed from all other runs in that the water was equilibrated with air for 1 week before the experiment was started, compared with less than 20 hours for all other runs. The latter explanation is more probable for all other runs, since if it is assumed that $1/k_E = 0$ in Equation 13 for runs 36, 39, and 40, these points conform well to the other data (Figure 10).

The mechanism of CO_2 release in gaseous form probably also occurred in most of the experiments carried out with water

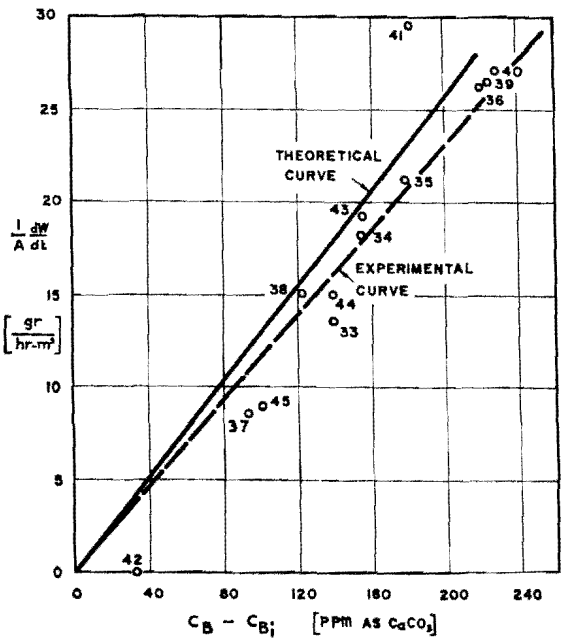

Figure 10. Effect of concentration on rate of growth with negligible CO_2 resistance for high concentration runs

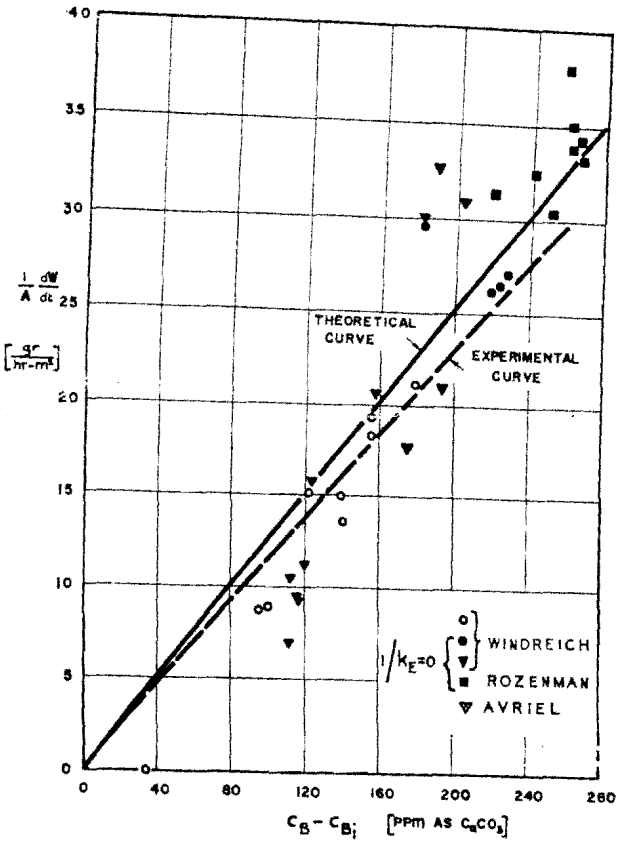

Figure 11. Correlation of all rate of growth results

supplied to the feed tank directly from the municipal supply. The very high supersaturation of dissolved CO_2 and the increased impurities in this water apparently led to release of gaseous CO_2 on the reaction surface. Assuming $1/k_E = 0$ for such runs, large differences in the growth-rate measurements obtained under seemingly identical conditions at various stages of this study (Avriel, 1963; Rozenman, 1965; Windreich, 1966) could be reconciled and reasonably correlated. This is shown in Figure 11, in which data relating to different velocities are brought to a common basis (25.5 cm. per second) according to the 0.68 power relationship of Equation 11.

Conclusions

This study elucidates the controlling mechanisms in $CaCO_3$ scale deposition on a heat-transfer surface under turbulent flow of nonboiling water containing dissolved scale constituents. The separate effects of basic parameters determining scale growth (flow velocity, scale surface temperature, and water composition) are examined according to the proposed rate mechanisms model.

Except under very low supersaturation conditions, nucleation on a scale-free metal surface is a negligible factor with $CaCO_3$ scale. Within the experimental range covered by this study (Reynolds numbers 13,000 to 42,000, surface temperature 67° to 85° C.), scale growth is controlled by the rate of forward diffusion of Ca^{+2} and HCO_3^- ions toward the scale-water interface. There are indications that the CO_2 formed during the reaction may either escape in gaseous form or may remain in solution, thus leading to lower scaling rates. The mechanism of CO_2 behavior on the reaction surface requires further investigation.

The constant heat-flux system developed in this work has been a valuable research tool for elucidating processes occurring in scale deposition. Further study of the dominant mechanisms controlling the formation and growth of the different scale substances under various conditions will provide the basic framework necessary for developing new and more efficient methods for overcoming the scaling problem.

Nomenclature

A = surface area of heated tube
C_B = bulk concentration of Ca^{+2} ions
C_{Bi} = concentration of Ca^{+2} ions at reaction interface
C_E = bulk concentration of dissolved CO_2
C_F = bulk concentration of HCO_3^- ions
C_p = specific heat of water
d_e = equivalent diameter of annular flow passage
h_i = water film coefficient for heat transfer
k, k' = rate coefficients for reversible bicarbonate decomposition reaction
k_{BF} = mass transfer coefficient for diffusion of Ca^{+2} ions (B), HCO_3^- ions (F), or $Ca(HCO_3)_2$ ($k_B = k_F = k_{BF}$)
k_E = mass transfer coefficient for diffusion of dissolved CO_2
k_R = rate coefficient for the crystallization "surface reaction"
k_s = thermal conductivity of scale
k_w = thermal conductivity of water
K_1' = first dissociation constant of carbonic acid, based on concentration units and taking into account ionic-strength effects
K_2' = second dissociation constant of carbonic acid, based on concentration units and taking into account ionic-strength effects
K_s' = solubility product of calcite, based on concentration units and taking into account ionic-strength effects
$(Pr)_f$ = Prandtl number of water, based on average film temperature
q = heat flow per unit time
$(Re)_f$ = Reynolds number of water, based on average film temperature
$(Sc)_f$ = Schmidt number, based on average film temperature [subscript BF refers to $Ca(HCO_3)_2$, subscript E refers to CO_2]
t = time
T_1 = inlet water temperature
T_b = bulk water temperature
T_o = wall temperature of heated copper tube
T_s = scale surface temperature
$w = \frac{1}{A} \cdot \frac{dW}{dT}$ = rate of growth of scale layer, weight per unit time per unit area
W' = mass flow rate of water
x = thickness of scale layer
ρ = density of water
ρ_s = density of scale

Literature Cited

Avriel, M., M.S. thesis, Chemical Engineering Department, Technion–Israel Institute of Technology, Haifa, Israel, 1963.
Hamer, P., Jackson, J., Thurston, E. F., "Industrial Water Treatment Practice," pp. 414–59, Butterworths, London, 1961.
Hasson, D., *Dechema Monograph.* **47**, 233 (1962).
Rothfus, R. R., Monrad, C. C., Sikchi, K. G., Heideger, W. G., *Ind. Eng. Chem.* **47**, 913 (1955).
Rozenman, T., M.S. thesis, Chemical Engineering Department, Technion–Israel Institute of Technology, Haifa, Israel, 1965.
Van Hook, A., "Crystallization," p. 115, Reinhold, New York, 1961.
Windreich, S., M.S. thesis, Chemical Engineering Department, Technion–Israel Institute of Technology, Haifa, Israel, 1966.

Received for review May 31, 1967
Accepted October 16, 1967

Second European Symposium on Fresh Water, Athens, Greece, May 1967. Part of theses submitted to the Senate of the Technion–Israel Institute of Technology, in partial fulfillment of the requirements for an M.S. degree. The authors are indebted to the Ford Foundation for supporting part of the work.